

# The influence of negatively charged heavy ions on the kinetic Alfvén wave in a cometary environment

Venugopal Chandu · E. Savithri Devi · R. Jayapal ·  
George Samuel · S. Antony · G. Renuka

Received: 15 March 2011 / Accepted: 28 December 2011 / Published online: 14 January 2012  
© Springer Science+Business Media B.V. 2012

**Abstract** Kinetic Alfvén waves are important in a wide variety of areas like astrophysical, space and laboratory plasmas. In cometary environments, waves in the hydromagnetic range of frequencies are excited predominantly by heavy ions. We, therefore, study the stability of the kinetic Alfvén wave in a plasma of hydrogen ions, positively and negatively charged oxygen ions and electrons. Each species was modeled by drifting ring distributions in the direction parallel to the magnetic field; in the perpendicular direction the distribution was simulated with a loss cone type distribution obtained through the subtraction of two Maxwellian distributions with different temperatures. We find that for frequencies  $\omega^* < \omega_{cH^+}$  ( $\omega^*$  and  $\omega_{cH^+}$  being respectively the Doppler shifted and hydrogen ion gyro-frequencies), the growth rate increases with increasing negatively charged oxygen ion densities while decreasing with increasing propagation angles, negative ion temperatures and negative ion mass.

**Keywords** Kinetic Alfvén wave · Stability · Multi-ion · Negative-ion cometary plasma

## 1 Introduction

Hydromagnetic wave activity has been observed in distinct space environments: in the distant magnetotail (Tsurutani

and Smith 1984), in the magnetosheath (Anderson et al. 1982), upstream of the Earth's (Hoppe et al. 1981) and other planets' bow shocks (Smith and Lee 1986) and upstream of interplanetary shocks (Tsurutani et al. 1983) especially near comets. In the space plasma environments nearer to our earth, Alfvén wave activity was frequently observed in the auroral regions by the spacecraft FREJA. The strong electric spikes associated with magnetic and density fluctuations were interpreted as kinetic Alfvén waves (KAWs) and were proposed as contributing to auroral plasma energization (Louarn et al. 1994). Other emissions in these regions also coincided with Alfvén wave activity from a few Hz to tens of Hz; these emissions were linked to the evolution of nonlinear KAWs (Wahlund et al. 1994a). Again, the broadband electrostatic turbulence identified as ion acoustic waves was thought of as evolving from solitary kinetic Alfvén waves (Wahlund et al. 1994b). A more recent evidence was the observation of small scale large amplitude KAWs/spikes at the plasma sheet boundary layer (PSBL), at altitudes of 4–6  $R_E$  (Wygant et al. 2002). Another example is the observation of the drift kinetic Alfvén wave in the vicinity of a reconnection X-line in the earth's magnetopause. These waves were observed to propagate outwards from the X-line suggesting that reconnection is a source of KAWs. Interestingly, energetic  $O^+$  observed in these waves indicate that reconnection is a driver of auroral ion outflow (Chaston et al. 2005).

Alfvén wave activity was also observed in cometary environments. Specifically, Alfvénic turbulence was detected in the magnetic field (Tsurutani and Smith 1986a, 1986b) and in the electron distribution (Gosling et al. 1986) at comet Giacobini-Zinner by the ICE spacecraft. Similar turbulence was also detected by Giotto (Neubauer et al. 1986) and Vega (Reidler et al. 1986) spacecrafts at comet Halley. In addition to these observations, Alfvénic turbulence was also observed

V. Chandu (✉) · E. Savithri Devi · R. Jayapal · G. Samuel ·  
S. Antony

School of Pure & Applied Physics, Mahatma Gandhi University,  
Priyadarshini Hills, Kottayam 686 560, Kerala, India  
e-mail: cvgmphys@yahoo.co.in

G. Renuka  
Department of Physics, University of Kerala, Kariavattom,  
Thiruvananthapuram 695 581, Kerala, India

in the solar wind protons and alpha particles, where the fluctuations were not only seen in the plasma velocity as expected for simple Alfvén waves, but also in the density and temperature as Giotto approached comet Halley (Johnstone et al. 1987).

Since the anticipation of Ip and Axford (1982) on theoretical grounds, of low frequency hydromagnetic turbulence upstream of a comet, possible excitation mechanisms emphasizing proton (or heavier) ion beams with Maxwellian (Gary et al. 1985) or drifting (Winske et al. 1985) velocity distributions were studied. While these studies were restricted to parallel propagation, oblique propagation was also considered (Sharma and Patel 1986). In particular, Gary and Sinha (1989) studied the stability of electromagnetic waves, below the proton cyclotron frequency, propagating parallel or anti-parallel to a uniform magnetic field. Brinca and Tsurutani (1989) studied numerically the oblique behavior of low frequency electromagnetic waves excited by cometary new born ions. Later, Killen et al. (1995) studied the excitation of obliquely propagating magnetosonic waves using a distribution function that represented a ring beam in the parallel direction and a delta function in the perpendicular direction, while Cao et al. (1998) investigated the oblique behavior of left circularly polarized electromagnetic waves driven by a ring of gyrotopical ions, again modeled by delta function distributions. In the analytical studies cited above, the thermal spreads of the particle distribution functions in the perpendicular direction were not considered. Besides, where applicable, these studies were confined to a plasma composition of hydrogen ions and electrons with only positively charged oxygen ions as the heavy ion component. However, negatively charged ions in three broad mass peaks of 7–19, 22–65 and 85–110 amu were observed in the coma of comet Halley. Of the many ionic components, negatively charged oxygen ( $O^-$ ) was unambiguously identified (Chaizy et al. 1991).

In general, a cometary environment contains hydrogen and new born heavier ions with relative densities depending on the distance from the nucleus, and each isolated beam capable of exciting instabilities. A model of the solar wind permeated by dilute, drifting ring distributions of electrons, hydrogen ions and positively charged oxygen ions with finite thermal spreads, was used to study numerically the electromagnetic waves excited by cometary new born ions (Brinca and Tsurutani 1987). In this model, the modes excited in the hydromagnetic frequency range were predominantly fed by the positively charged heavier oxygen ions.

We have, therefore, studied the stability of the kinetic Alfvén wave in a plasma of hydrogen ions, positively and negatively charged oxygen ions and electrons. Each species

has been modeled by a drifting ring distribution in the direction parallel to the magnetic field. In the direction perpendicular to the magnetic field, another ring was simulated with a loss cone type distribution obtained by the subtraction of two Maxwellians with different temperatures (Brinca and Tsurutani 1987). Analytic expressions were derived both for the real part of the dispersion relation as well as the growth/damping rate. However, since we are interested in a study over a wide range of parameters, the dispersion relation was solved numerically. It was found that for frequencies  $\omega^* < \omega_{cH^+}$  ( $\omega^*$  and  $\omega_{cH^+}$  being, respectively, the Doppler shifted and the hydrogen ion-gyro frequencies), the growth rate increased with increasing negative oxygen ion densities and decreased with increasing propagation angles, negative ion temperatures and negative ion mass.

## 2 The elements of the dielectric tensor

As mentioned above, we are interested in the stability of the kinetic Alfvén wave in a plasma of hydrogen ions ( $H^+$ ), positively and negatively charged oxygen ions ( $O^+$  and  $O^-$  respectively) and electrons ( $e$ ), with each species being modeled by drifting ring distributions in the direction parallel to the magnetic field. Another ring, simulated by a loss-cone type distribution, was obtained by subtracting two Maxwellians with different temperatures. This distribution function is given by (Brinca and Tsurutani 1987)

$$F_s(v_\perp, v_\parallel) = f_{\perp s}(v_\perp) f_{\parallel s}(v_\parallel) \quad \text{where}$$

$$f_{\parallel s}(v_\parallel) = \frac{1}{\sqrt{\pi} v_{ts}} \exp\left[-\left(\frac{v_\parallel - V_{sw} \cos \alpha}{v_{ts}}\right)^2\right] \quad \text{and} \quad (1)$$

$$f_{\perp s}(v_\perp) = \frac{1}{\pi (a_s - b_s) v_{ts}^2} \left[ \exp\left(-\frac{v_\perp^2}{a_s v_{ts}^2}\right) - \exp\left(-\frac{v_\perp^2}{b_s v_{ts}^2}\right) \right] \quad a_s > b_s \quad (2)$$

In the above  $V_{sw}$  and  $v_{ts}$  are respectively the velocity of the solar wind and thermal velocity of species ' $s$ ' ( $=H^+$ ,  $O^+$ ,  $O^-$  or  $e$ );  $\alpha$  is the pitch angle.

The elements of the dielectric tensor required for the derivation of the dispersion relation of the kinetic Alfvén wave are given by (Krall and Trivelpiece 1973; Shukla et al. 2007)

$$D_{xx} = 1 - \frac{c^2 k_\parallel^2}{\omega^2} + \sum_s \frac{\omega_{ps}^2}{\omega} \sum_n \int d^3 v v_\perp \frac{(n^2 J_n^2(y_s))}{y_s^2 (\omega - n\omega_{cs} - k_\parallel v_\parallel)} \times \left[ \frac{\partial F_s}{\partial v_\perp} - \frac{k_\parallel v_\parallel}{\omega} \left( \frac{\partial F_s}{\partial v_\perp} - \frac{v_\perp}{v_\parallel} \frac{\partial F_s}{\partial v_\parallel} \right) \right] \quad (3)$$

$$D_{xz} = \frac{c^2 k_{\parallel} k_{\perp}}{\omega^2} + \sum_s \frac{\omega_{ps}^2}{\omega} \sum_n \int d^3 v v_{\perp} \frac{(n J_n^2(y_s))}{y_s (\omega - n \omega_{cs} - k_{\parallel} v_{\parallel})} \times \left[ \frac{\partial F_s}{\partial v_{\parallel}} + \frac{n \omega_{cs}}{\omega} \left( \frac{v_{\parallel}}{v_{\perp}} \frac{\partial F_s}{\partial v_{\perp}} - \frac{\partial F_s}{\partial v_{\parallel}} \right) \right] \tag{4}$$

$$D_{zx} = \frac{c^2 k_{\parallel} k_{\perp}}{\omega^2} + \sum_s \frac{\omega_{ps}^2}{\omega} \sum_n \int d^3 v v_{\parallel} \frac{(n J_n^2(y_s))}{y_s (\omega - n \omega_{cs} - k_{\parallel} v_{\parallel})} \times \left[ \frac{\partial F_s}{\partial v_{\perp}} - \frac{k_{\parallel} v_{\parallel}}{\omega} \left( \frac{\partial F_s}{\partial v_{\perp}} - \frac{v_{\perp}}{v_{\parallel}} \frac{\partial F_s}{\partial v_{\parallel}} \right) \right] \tag{5}$$

and

$$D_{zz} = 1 - \frac{c^2 k_{\perp}^2}{\omega^2} + \sum_s \frac{\omega_{ps}^2}{\omega} \sum_n \int d^3 v v_{\parallel} \frac{(J_n^2(y_s))}{(\omega - n \omega_{cs} - k_{\parallel} v_{\parallel})} \times \left[ \frac{\partial F_s}{\partial v_{\parallel}} + \frac{n \omega_{cs}}{\omega} \left( \frac{v_{\parallel}}{v_{\perp}} \frac{\partial F_s}{\partial v_{\perp}} - \frac{\partial F_s}{\partial v_{\parallel}} \right) \right] \tag{6}$$

with the dispersion relation being given by

$$D_{xx} D_{zz} - D_{xz} D_{zx} = 0 \tag{7}$$

In (3) to (6), ‘s’ indicates a summation over the species (= H, O<sup>+</sup>, O<sup>-</sup> or e),  $\omega_{ps} = (4\pi n_{0s} e^2 / m_s)^{1/2}$  is the corresponding plasma frequency while  $\omega_{cs} = |e| B_0 / (m_s c)$  is the gyro-frequency. Also  $\int d^3 v = \int 2\pi v_{\perp} dv_{\perp} dv_{\parallel}$  and  $y_s = k_{\perp} v_{\perp} / \omega_{cs}$  while  $k_{\perp}$  and  $k_{\parallel}$  are, respectively, the wave vectors perpendicular and parallel to the magnetic field. All the other terms in (3) to (6) have their usual meaning.

Substituting (1) and (2) into (3) to (6) and carrying out the  $dv_{\parallel}$  integration using the plasma dispersion function (Fried and Conte 1961)

$$Z(\zeta) = \frac{1}{\sqrt{\pi}} \int \frac{\exp(-x^2)}{x - \zeta} dx \tag{8}$$

and the  $dv_{\perp}$  integrations using the basic form

$$\begin{aligned} & \int_0^{\infty} \exp(-x^2/v_t^2) J_n(\alpha x) J_n(\beta x) x dx \\ &= \frac{v_t^2}{2} \exp\left[-\frac{(\alpha^2 + \beta^2)v_t^2}{4}\right] I_n\left(\frac{\alpha\beta v_t^2}{2}\right) \\ &= \frac{v_t^2}{2} \Lambda_n \end{aligned} \tag{9}$$

we get the final expressions for the elements of the dielectric tensor as

$$D_{xx} = 1 - \frac{c^2 k_{\parallel}^2}{\omega^2} + \sum_s \frac{\omega_{ps}^2}{\omega^2} \times \sum_n n^2 \left\{ \chi_n \left[ \left( \frac{\omega - k_{\parallel} V_{sw} \cos \alpha}{k_{\parallel} v_{ts}} \right) Z(\zeta_s) - (1 + \zeta_s Z(\zeta_s)) \right] + \phi_n (1 + \zeta_s Z(\zeta_s)) \right\}$$

$$D_{xz} = \frac{c^2 k_{\parallel} k_{\perp}}{\omega^2} + \frac{k_{\perp}}{k_{\parallel}} \sum_s \frac{\omega_{ps}^2}{\omega^2} \sum_n \left\{ n^2 \chi_n \left[ 1 + \left( \zeta_s + \frac{V_{sw} \cos \alpha}{v_{ts}} \right) Z(\zeta_s) \right] + \frac{n(\omega - n \omega_{cs})}{\omega_{cs}} \phi_n (1 + \zeta_s Z(\zeta_s)) \right\}$$

$$D_{zx} = \frac{c^2 k_{\parallel} k_{\perp}}{\omega^2} + \sum_s \frac{\omega_{ps}^2}{\omega^2} \sum_n \left\{ \frac{k_{\perp}}{k_{\parallel}} \frac{\omega}{\omega_{cs}} n \chi_n \times \left[ 1 + \zeta_s Z(\zeta_s) + \frac{V_{sw} \cos \alpha}{v_{ts}} Z(\zeta_s) \right] - \frac{k_{\perp} v_{ts}}{\omega_{cs}} n \chi_n \left[ (1 + \zeta_s Z(\zeta_s)) \left( \zeta_s + 2 \frac{V_{sw} \cos \alpha}{v_{ts}} \right) + \left( \frac{V_{sw} \cos \alpha}{v_{ts}} \right)^2 Z(\zeta_s) \right] + \frac{n \omega_{cs}}{k_{\perp} v_{ts}} \left( \frac{\omega - n \omega_{cs}}{k_{\parallel} v_{ts}} \right) L_{\perp s} \phi_n (1 + \zeta_s Z(\zeta_s)) \right\} \tag{10}$$

$$D_{zz} = 1 - \frac{c^2 k_{\perp}^2}{\omega^2} + 2 \sum_s \frac{\omega_{ps}^2}{\omega^2} \sum_n \left\{ \frac{n \omega_{cs}}{k_{\parallel} v_{ts}} L_{\perp s} \chi_n \times \left[ (1 + \zeta_s Z(\zeta_s)) \left( \zeta_s + 2 \frac{V_{sw} \cos \alpha}{v_{ts}} \right) + \left( \frac{V_{sw} \cos \alpha}{v_{ts}} \right)^2 Z(\zeta_s) \right] + \left( \frac{\omega - n \omega_{cs}}{k_{\parallel} v_{ts}} \right)^2 \times L_{\perp s} \phi_n (1 + \zeta_s Z(\zeta_s)) \right\}$$

In relations (10)

$$\chi_n = \frac{\Lambda_n (a_s L_{\perp s}) - \Lambda_n (b_s L_{\perp s})}{(a_s - b_s) L_{\perp s}} \tag{11}$$

and

$$\phi_n = \frac{a_s \Lambda_n (a_s L_{\perp s}) - b_s \Lambda_n (b_s L_{\perp s})}{(a_s - b_s) L_{\perp s}} \tag{12}$$

with  $L_{\perp s} = k_{\perp}^2 v_{ts}^2 / (2\omega_{cs}^2)$ . Equations (11) and (12) are functions of the modified Bessel function  $I_n$  of order  $n$  through (9) and argument  $L_{\perp s}$ . The argument  $\zeta_s$  of the dispersion function  $Z(\zeta_s)$  is

$$\zeta_s = \frac{\omega - k_{\parallel} V_{sw} \cos \alpha - n \omega_{cs}}{k_{\parallel} v_{ts}} = \frac{\omega^* - n \omega_{cs}}{k_{\parallel} v_{ts}} \tag{13}$$

### 3 The dispersion relation

In this section we use the dispersion formula (7) and the elements of the dielectric tensor (10) to arrive at the dispersion relation for the kinetic Alfvén wave in the frequency regime  $\omega^* \ll \omega_{cH^+}$ .

We use the asymptotic expansion for the plasma dispersion function which is given by  $Z(\zeta_s) = -\frac{1}{\zeta_s} - \frac{1}{2\zeta_s^3} - \dots + i\sqrt{\pi} \exp(-\zeta_s^2)$  (Fried and Conte 1961). Only the  $n = \pm 1$  ion terms contribute to  $D_{xx}$ . The dominant contribution to  $D_{zz}$  is from the  $n = 0$  electron term. The simplified final expressions for the tensor elements are:

$$\begin{aligned}
 D_{xx} &\approx \frac{\omega_{pH^+}^2}{\omega_{cH^+}^2} \frac{\omega^{*2}}{\omega^2} (2\chi_1)_{H^+} \\
 &\quad - \frac{\omega_{pO^+}^2}{\omega^2} (2\chi_1)_{O^+} - \frac{\omega_{pO^-}^2}{\omega^2} (2\chi_1)_{O^-} - \frac{c^2 k_{\parallel}^2}{\omega^2} \\
 D_{xz} = D_{zx} &\approx \frac{c^2 k_{\parallel} k_{\perp}}{\omega^2} \quad \text{and} \\
 D_{zz} &\approx -\frac{\omega_{pe}^2}{\omega^{*2}} L_{\perp e}(\phi)_e + 2i\sqrt{\pi} \frac{\omega_{pe}^2 \omega^* L_{\perp e}}{(k_{\parallel} v_{te})^3} (\phi)_e e^{-\zeta_{0e}^2} \\
 &\quad - \frac{c^2 k_{\perp}^2}{\omega^2}
 \end{aligned}
 \tag{14}$$

Substituting (14) into (7) and simplifying and assuming that  $c^2 k^2 / \omega_{pe}^2 \ll 1$  we get the real part of the dispersion relation for the kinetic Alfvén wave as

$$\begin{aligned}
 \omega^{*2} &= \frac{k_{\parallel}^2 v_A^2 + \frac{n_{O^+}}{n_{H^+}} \omega_{cO^+} \omega_{cH^+} (2\chi_1)_{O^+}}{(2\chi_1)_{H^+}} \\
 &\quad + \frac{\frac{n_{O^-}}{n_{H^+}} \omega_{cO^-} \omega_{cH^+} (2\chi_1)_{O^-}}{(2\chi_1)_{H^+}}
 \end{aligned}
 \tag{15}$$

In (15)  $n_{H^+}$ ,  $n_{O^+}$  and  $n_{O^-}$  are, respectively, the equilibrium densities of the hydrogen ions and positively and negatively charged oxygen ions, while  $v_A$  is the Alfvén velocity defined by  $v_A = B_0 / \sqrt{4\pi n_{H^+} m_{H^+}}$ .

Putting  $\omega^* = \omega_r^* + i\Gamma$  and simplifying we get the final expression for the growth/damping rate as

$$\begin{aligned}
 \Gamma &= \frac{\sqrt{\pi}}{(2\chi_1)_{H^+}} \frac{(\omega_r^*)^2}{(k_{\parallel} v_{te})^3} e^{-\zeta_{0e,r}^{*2}} \left[ (\omega_r^*)^2 (2\chi_1)_{H^+} \right. \\
 &\quad \left. - k_{\parallel}^2 v_A^2 - \sum_{j=O^+,O} \frac{n_j}{n_{H^+}} \omega_{cH^+} \omega_{cj} (2\chi_1)_j \right]
 \end{aligned}
 \tag{16}$$

### 4 Discussion

The dispersion relation (15) and the expression for the growth/damping rate (16) are very general relations. For example, (15) reduces to the well known dispersion relation  $\omega^2 = k_{\parallel}^2 v_A^2$  when the heavy ion densities and  $V_{sw}$  are zero. In fact, (15) closely resembles the dispersion relation

of Hasegawa and Chen (1975) which was for a single ion plasma. In their study, Hasegawa and Chen (1975) found that heating of the plasma occurred as a result of the damping of the modified Alfvén wave by finite Larmor radius effects. It may be noted that the dispersion relation (15) is now modified by the finite Larmor radius effects of all three types of ions. Another interesting feature is the modification of both the dispersion relation and the growth/damping rate by the ion-ion hybrid resonances between the majority species  $H^+$  and the minority, heavier ion species  $O^+$  and  $O^-$ .

In a three fluid model study of KAWs in a hydrogen-oxygen-electron plasma (Yang and Wu 2005) it was found that the parallel phase speed of the KAW in one of the solutions was much larger than the Alfvén velocity in the presence of heavy ions in the plasma. From (15) it is obvious that both  $O^+$  and  $O^-$  contribute to an increase in the parallel phase velocity. This phenomenon is interesting as KAWs can then produce a more effective acceleration of particles (Yang and Wu 2005).

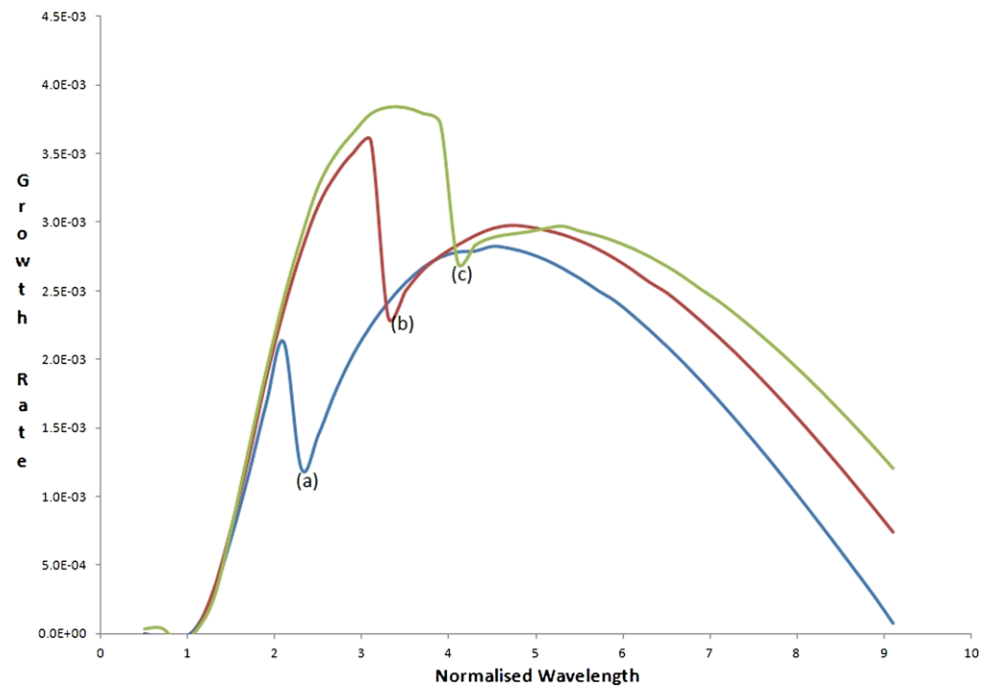
Next consider relation (16), the expression for the growth/damping rate. For simplicity if we put the oxygen ion densities  $n_{O^+} = n_{O^-} = 0$  and the solar wind velocity  $V_{sw} = 0$ , the wave can grow only if its phase velocity  $\omega/k_{\parallel}$  is greater than the Alfvén velocity; that is in regions where the magnetic field is weak. For  $V_{sw} \neq 0$ , the wave can also grow in regions where the solar wind velocity is large; that is, when  $V_{sw} \gg v_A$  or when we have a beam like condition with the kinetic energy of the particles being large. On the other hand, when  $\omega/k_{\parallel} \approx V_{sw} \cos \alpha$ , the wave is likely to be damped since the term  $(k_{\parallel} v_A)^2$  is likely to dominate. In other words, the wave is more likely to be damped in regions where the magnetic field is strong.

### 5 Results

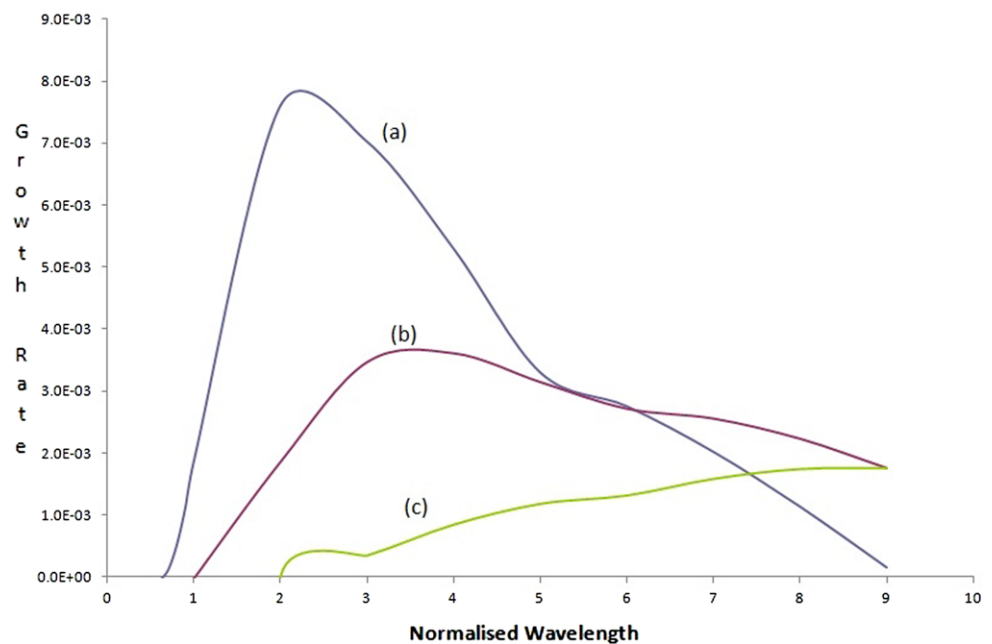
Since we intend to study the growth/damping rates over a wide range of parameters, we have solved the dispersion relation numerically. The dispersion relation which was set up using the dispersion formula (7) and the tensor elements (10) was solved using a subroutine based on Muller’s method (Press et al. 1993) for the same parameters as in Brinca and Tsurutani (1987). The parameters common to all the figures are  $n_{H^+} = 4.95 \text{ cm}^{-3}$ ,  $a_s = 1.8$ ,  $b_s = 1.2$ , with the temperatures and positively charged oxygen ion density slightly higher at  $T_e = 1 \times 10^6 \text{ K}$ ,  $T_{H^+} = 9 \times 10^5 \text{ K}$  and  $T_{O^+} = 1.2 \times 10^3 \text{ K}$  and  $n_{O^+} = 0.5 \text{ cm}^{-3}$ . As a simplifying assumption we set  $T_{O^+} = T_{O^-}$  in all figures except Fig. 3.

Figure 1 is a plot of the normalized growth rate  $\Gamma/\omega_{cH^+}$  versus  $k_{\perp} r_{LH^+}$  ( $r_{LH^+}$  being the hydrogen ion Larmor radius) for the parameters given above and a propagation angle  $\vartheta = 70^\circ$  as a function of the negatively charged oxygen ion density  $n_{O^-}$ . Curve (a) is for  $n_{O^-} = 0$ , curve (b) is

**Fig. 1** Plot of the normalized growth  $\Gamma/\omega_{cH^+}$  versus  $k_{\perp}r_{LH^+}$  for  $n_{H^+} = 4.95 \text{ cm}^{-3}$ ,  $a_s = 1.8$ ,  $b_s = 1.2$ ,  $n_{O^+} = 0.5 \text{ cm}^{-3}$ ,  $T_e = 1 \times 10^6 \text{ K}$ ,  $T_{H^+} = 9 \times 10^5 \text{ K}$  and  $T_{O^+} = T_{O^-} = 1.2 \times 10^3 \text{ K}$  as a function of the negatively charged oxygen ion density. The propagation angle  $\vartheta = 70^\circ$ . Curve (a) is for  $n_{O^-} = 0$ , curve (b) is for  $n_{O^-} = 0.1 \text{ cm}^{-3}$  and curve (c) is for  $n_{O^-} = 0.2 \text{ cm}^{-3}$



**Fig. 2** Plot of the normalized growth  $\Gamma/\omega_{cH^+}$  versus  $k_{\perp}r_{LH^+}$  as a function of the propagation angle  $\vartheta$ . Curve (a) is for  $\vartheta = 65^\circ$ , curve (b) is for  $\vartheta = 70^\circ$  and curve (c) is for  $\vartheta = 75^\circ$ . The negatively charged oxygen ion density  $n_{O^-} = 0.4 \text{ cm}^{-3}$ , while the other parameters are the same as in Fig. 1



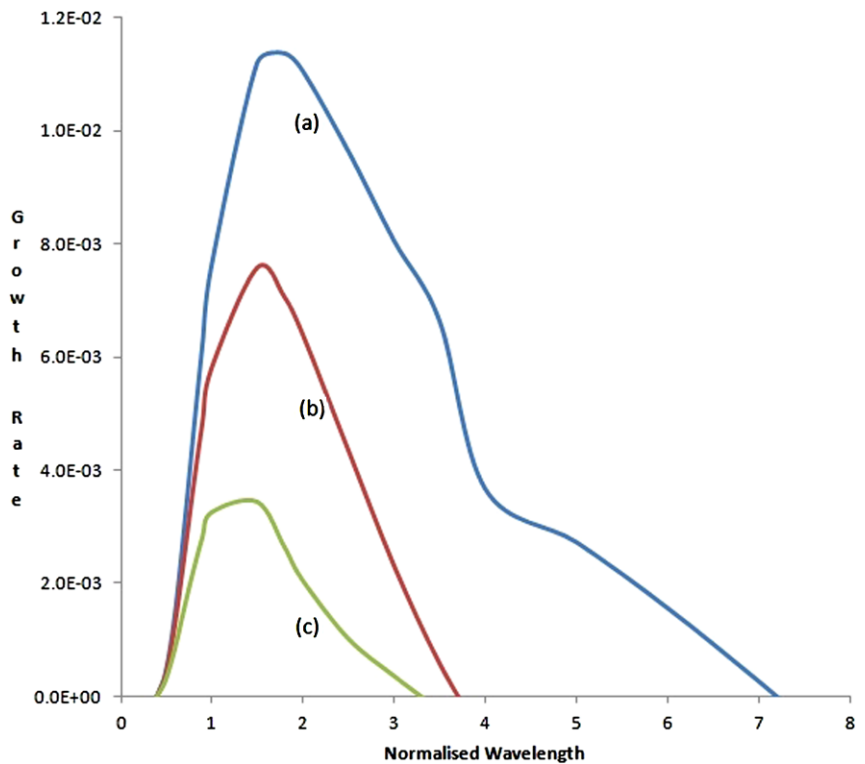
for  $n_{O^-} = 0.1 \text{ cm}^{-3}$  and curve (c) is for  $n_{O^-} = 0.2 \text{ cm}^{-3}$ . It is evident from the curves that the growth which starts from low values reaches a maximum and then gradually approaches zero as  $k_{\perp}r_{LH^+}$  increases. Also it increases with increasing negatively charged oxygen ion densities  $n_{O^-}$ . This result is also in agreement with the earlier conclusion that the modes excited in the hydromagnetic frequency range were predominantly fed by positively charged oxygen ions

(Brinca and Tsurutani 1987): our results indicate that  $O^-$  ions also contribute to the instability.

Figure 2 is also a plot of the normalized growth rate  $\Gamma/\omega_{cH^+}$  versus  $k_{\perp}r_{LH^+}$  but as a function of the propagation angle  $\vartheta$  with  $n_{O^-} = 0.4 \text{ cm}^{-3}$ , while the other parameters are the common parameters given above. Curve (a) is for  $\vartheta = 65^\circ$ , curve (b) for  $\vartheta = 70^\circ$  and curve (c)  $\vartheta = 75^\circ$ . While the curves are similar to that in Fig. 1, it is seen that the growth rate decreases with increasing propagation an-



**Fig. 3** Plot of the normalized growth rate  $\Gamma/\omega_{cH^+}$  versus  $k_{\perp}r_{LH^+}$  as a function of the negatively charged oxygen ion temperature. The propagation angle  $\vartheta = 60^\circ$  and the negatively charged oxygen ion density  $n_{O^-} = 0.4 \text{ cm}^{-3}$ . Curve (a) is for  $T_{O^-} = 1.2 \times 10^3 \text{ K}$ , curve (b) is for  $T_{O^-} = 4.8 \times 10^3 \text{ K}$  and curve (c) is for  $T_{O^-} = 9.6 \times 10^3 \text{ K}$ ; other parameters are the same as in Figs. 1 and 2



gle  $\vartheta$ . This could be due to the fact that the influence of the solar wind, which is assumed propagating parallel to the magnetic field, decreases as we go towards perpendicular propagation.

It may be noted here that a large number of solitary KAW events were observed with their propagation angles in the range of  $50^\circ$  to  $70^\circ$  in the magnetosphere by the satellite FREJA. Also the phase velocities of these waves generally decreased as the propagation angle increased (Huang et al. 1997). For a given wavelength, a decrease in the phase velocity is due to a decrease in the frequency  $\omega$ . Since  $\omega = \omega_r + i\Gamma$ , the decrease in the growth rate with increasing propagation angles, as depicted in Fig. 2, is consistent with the observed results.

The growth rate was also studied as a function of the temperature of the  $O^-$  ions. Thus Fig. 3 is a plot of the normalized growth rate  $\Gamma/\omega_{cH^+}$  versus  $k_{\perp}r_{LH^+}$  as a function of the negatively charged oxygen ion temperature. The propagation angle  $\vartheta = 60^\circ$  and the negatively charged oxygen ion density  $n_{O^-} = 0.4 \text{ cm}^{-3}$ ; the other parameters are the same as in Figs. 1 and 2. Curve (a) is for  $T_{O^-} = 1.2 \times 10^3 \text{ K}$ , curve (b) is for  $T_{O^-} = 4.8 \times 10^3 \text{ K}$  and curve (c) is for  $T_{O^-} = 9.6 \times 10^3 \text{ K}$ ; we find that the growth rate decreases as the negative ion temperature increases.

The growth rate was also studied as a function of the parameter  $b_s$ , which is a measure of the number of particles missing from the distribution function. Thus the theoretical limits of  $b_s \rightarrow 0$  and  $b_s \rightarrow \infty$  correspond, respectively, to a minimum and maximum number of particles missing from

the plasma. Figure 4 is thus a plot  $\Gamma/\omega_{cH^+}$  versus  $k_{\perp}r_{LH^+}$  as a function of  $b_s$ , with  $a_s = 2.7$ , propagation angle  $\vartheta = 60^\circ$ ,  $n_{O^-} = 0.4 \text{ cm}^{-3}$ , while the other temperatures and densities remain unchanged. Curve (a) is for  $b_s = 1.8$ , curve (b) for  $b_s = 2.0$  and curve (c) for  $b_s = 2.5$ ; we find that there is a slight decrease in the growth rate as  $b_s$  increases. Physically this could be due to the fact that there is a slight decrease in the number of particles (as  $b_s$  increases) from which the wave can absorb energy and grow.

Besides  $O^-$ , a number of other negatively charged ions were also observed. Among others, the prominent ones were  $OH^-$ ,  $CH^-$ ,  $CN^-$ , etc. (Chaizy et al. 1991). Figure 5 is thus a plot of the growth rate versus  $k_{\perp}r_{LH}$ , with  $O^-$  and  $CN^-$ . To explore the effect of the larger mass, we adopted the same values of density and temperature for both types of ions, namely  $n_{O^-} = n_{CN^-} = 0.4 \text{ cm}^{-3}$  and  $T_{O^-} = T_{CN^-} = 1.2 \times 10^3 \text{ K}$ , the  $a_s$  and  $b_s$  values, the densities and temperatures of electrons,  $H^+$  and  $O^+$  remaining the same as in Figs. 1–3. The propagation angle  $\vartheta = 60^\circ$ . Curve (a) depicts the growth rate when the heavier ion is  $O^-$  and curve (b) when the heavier ion is  $CN^-$ . As can be seen there is a clear reduction in the growth rate when the heavier ion is  $CN^-$ . Since the temperatures of both these ions were assumed the same, the reduction in the growth rate for  $CN^-$  could be due to the lower thermal velocity of these ions as compared to  $O^-$ . This result could be of relevance nearer earth as negative pickup ions were occasionally detected during the Tethered Satellite System mission of the

**Fig. 4** Plot of the normalized growth rate  $\Gamma/\omega_{cH^+}$  versus  $k_{\perp}r_{LH^+}$  as a function of the parameter  $b_s$  of the distribution function. The propagation angle  $\vartheta = 60^\circ$ ,  $a_s = 2.7$  and  $n_{O^-} = 0.4 \text{ cm}^{-3}$ . Curve (a) is for  $b_s = 1.8$ , curve (b) is for  $b_s = 2.0$  and curve (c) is for  $b_s = 2.5$ ; other densities and temperatures are the same as in Figs. 1 and 2

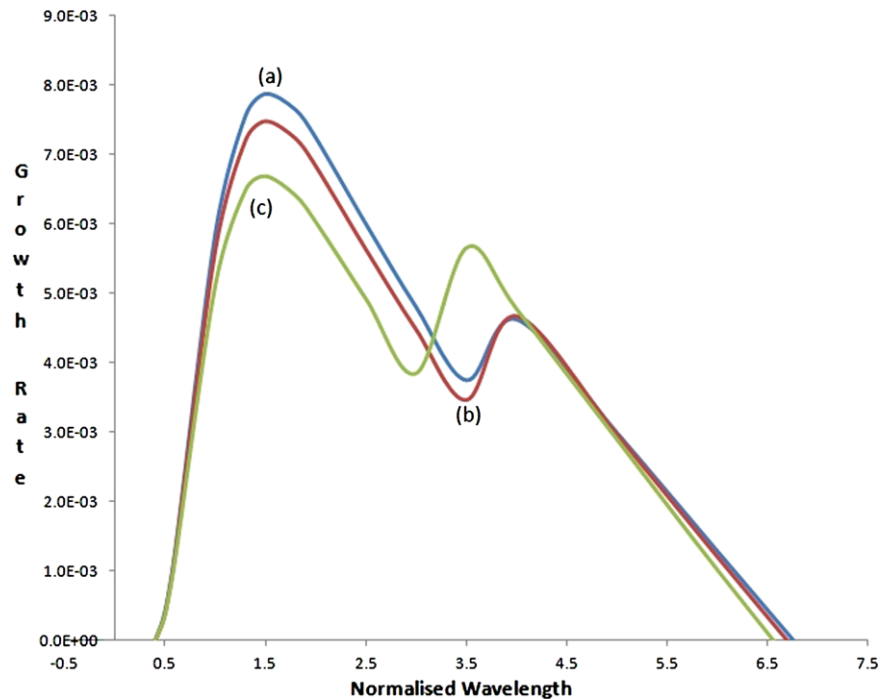
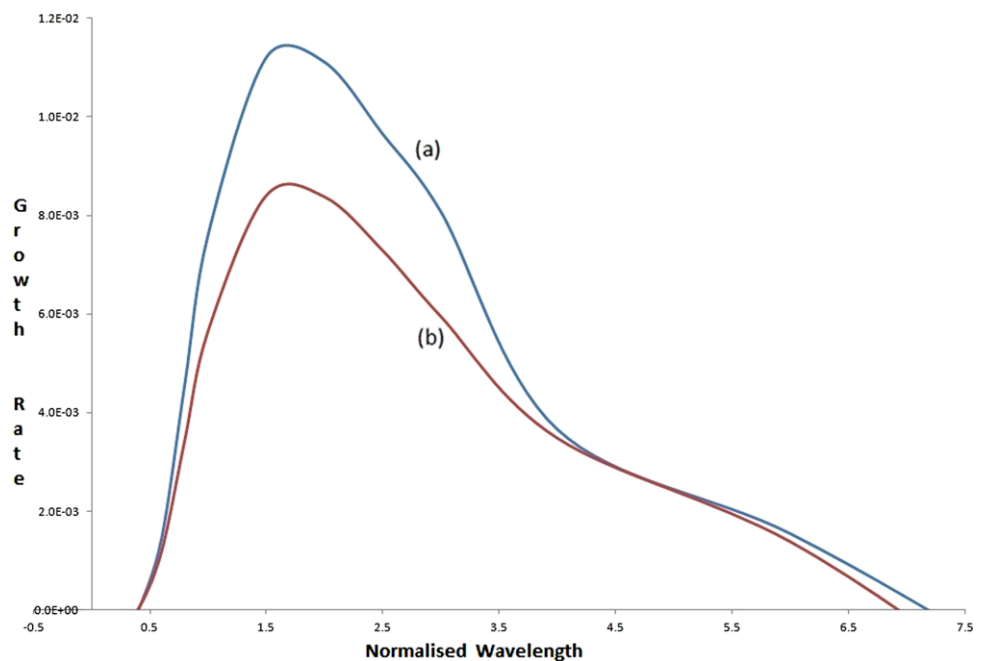


**Fig. 5** Plot of the normalized growth rate  $\Gamma/\omega_{cH^+}$  versus  $k_{\perp}r_{LH^+}$  as a function of the negative ion mass: Curve (a) is when the heavier negative ion is  $O^-$  with  $n_{O^-} = 0.4 \text{ cm}^{-3}$ ,  $T_{O^-} = 1.2 \times 10^3 \text{ K}$  and curve (b) when the heavier negative ion is  $CN^-$  with  $n_{CN^-} = 0.4 \text{ cm}^{-3}$ ,  $T_{CN^-} = 1.2 \times 10^3 \text{ K}$ . The propagation angle  $\vartheta = 60^\circ$  while the other parameters are the same as in Fig. 1



Space Shuttle. The negative ions were identified as  $NO_2^-$  or  $MMH^-$  (Rubin et al. 1997).

## 6 Conclusions

We have, in this paper, studied the stability of the kinetic Alfvén wave in a plasma composed of hydrogen ions, positively and negatively charged oxygen ions and electrons. All

species of particles were modeled by distribution functions that could be separated into a drifting Maxwellian distribution in the direction parallel to the magnetic field; in the perpendicular direction the distribution functions were of the loss-cone type obtained by subtracting two Maxwellian distributions. It is found that for frequencies  $\omega^* < \omega_{cH^+}$  ( $\omega^*$  and  $\omega_{cH^+}$  being respectively the Doppler shifted and the hydrogen ion-gyro frequencies), the growth rate increased with increasing negative oxygen ion densities; it also decreased

with increasing propagation angles,  $O^-$  temperatures and negative ion mass.

**Acknowledgements** The authors enthusiastically thank the referee for bringing to their attention a number of relevant references and also for the very enlightening comments which have vastly improved the contents of the paper. CVG and SA acknowledge financial assistance from the University Grants Commission (Special Assistance Program) and Department of Science and Technology (PURSE Program). JR and SDE thank the University Grants Commission for a Teacher and Junior Fellowship respectively.

## References

- Anderson, R.R., Harvey, C.C., Hoppe, M.M., Tsurutani, B.T., Eastman, T.E., Etcheto, J.J.: *J. Geophys. Res.* **87**, 2082 (1982)
- Brinca, A.L., Tsurutani, B.T.: *Astron. Astrophys.* **187**, 311 (1987)
- Brinca, A.L., Tsurutani, B.T.: *J. Geophys. Res.* **94**, 3 (1989)
- Cao, J.B., Mazelle, C., Belmont, G., Reme, H.: *J. Geophys. Res.* **103**, 2055 (1998)
- Chaizy, P.H., Reme, H., Sauvaud, J.A., et al.: *Nature* **349**, 343 (1991)
- Chaston, C.C., Phan, T.D., Bonnell, J.W., Mozer, F.S., Acuna, M., Goldstein, M.L., Balogh, A., Andre, M., Reme, H., Fazakerley, A.: *J. Geophys. Res.* **110**, A02211 (2005). doi:[10.1029/2004JA010483](https://doi.org/10.1029/2004JA010483)
- Fried, F.B., Conte, S.D.: *The Plasma Dispersion Function*. Academic Press, New York (1961)
- Gary, S.P., Sinha, R.: *J. Geophys. Res.* **94**, 9131 (1989)
- Gary, S.P., Madland, C.D., Tsurutani, B.T.: *Phys. Fluids* **28**, 3691 (1985)
- Gosling, J.T., Asbridge, J.R., Bame, S.J., Thomsen, M.F., Zwickl, R.D.: *Geophys. Res. Lett.* **13**, 267 (1986)
- Hasegawa, A., Chen, L.: *Phys. Rev. Lett.* **35**, 370 (1975)
- Hoppe, M.M., Russel, C.T., Frank, L.A., Eastman, T.E., Greenstadt, E.W.: *J. Geophys. Res.* **86**, 4471 (1981)
- Huang, G.L., Wang, D.Y., Wu, D.J., de Feraudy, H., le Queau, D., Volwerk, M., Holback, B.: *J. Geophys. Res.* **102**, 7217 (1997)
- Ip, W.H., Axford, W.I.: In: Wilkening, L.L. (ed.) *Comets*, p. 588. Univ. Arizona Press, Tuscon (1982)
- Johnstone, A., Glassmeier, K., Acuna, M., et al.: *Astron. Astrophys.* **187**, 47 (1987)
- Krall, N.A., Trivelpiece, A.W.: *Principles of Plasma Physics*, p. 349. San Francisco Press, San Francisco (1973)
- Killen, K., Omid, N., Krauss-Varban, D., Karimabadi, H.: *J. Geophys. Res.* **100**, 5835 (1995)
- Neubauer, F., Glessmeier, K., Pohl, M., et al.: *Nature* **321**, 352 (1986)
- Louarn, P., Wahlund, J.E., Chust, T., de Feraudy, H., Roux, A., Holback, A., Dovner, P.O., Eriksson, A.I., Holmgren, G.: *Geophys. Res. Lett.* **21**, 1847 (1994)
- Press, W.H., Teukolsky, S.A., Vetterling, W.T., Flannery, B.P.: *Numerical Recipes in FORTRAN: The art of Scientific Computing*, 2nd edn. Foundation Books, New Delhi (1993)
- Rubin, A.G., Burke, W.J., Hardy, D.A., Huang, C.Y., Gentile, L.C., Hunton, D.E.: *J. Geophys. Res.* **102**, 4623 (1997)
- Reidler, W., Schwingenschuh, K., Yeroshenko, Y.G., Styashkin, V.A., Russel, C.T.: *Nature* **321**, 288 (1986)
- Sharma, O., Patel, V.: *J. Geophys. Res.* **91**, 1529 (1986)
- Shukla, N., Varma, P., Tiwari, M.S.: *J. Plasma Phys.* **73**, 911 (2007)
- Smith, C.W., Lee, M.A.: *J. Geophys. Res.* **91**, 81 (1986)
- Tsurutani, B.T., Smith, E.J.: *Geophys. Res. Lett.* **11**, 331 (1984)
- Tsurutani, B.T., Smith, E.J.: *Geophys. Res. Lett.* **13**, 259 (1986a)
- Tsurutani, B.T., Smith, E.J.: *Geophys. Res. Lett.* **13**, 263 (1986b)
- Tsurutani, B.T., Smith, E.J., Jones, D.E.: *J. Geophys. Res.* **88**, 5645 (1983)
- Wahlund, J.E., Louarn, P., Chust, T., de Feraudy, H., Holback, B., Cabrit, B., Eriksson, A.I., Kitner, P.M., Kelley, M.C., Bonnell, J., Chesney, S.: *Geophys. Res. Lett.* **21**, 1835 (1994a)
- Wahlund, J.E., Louarn, P., Chust, T., de Feraudy, H., Roux, A., Holback, B., Dovner, P.O., Holmgren, S.: *Geophys. Res. Lett.* **21**, 1831 (1994b)
- Winske, D., Wu, C.S., Li, Y.Y., Mou, Z.Z., Guo, S.Y.: *J. Geophys. Res.* **90**, 2713 (1985)
- Wygant, J.R., Keiling, A., Cattell, C.A., Lysak, R.L., Temerin, M., Mozer, F.S., Kletzing, C.A., Scudder, J.D., Stretsov, V., Lotko, W., Russell, C.T.: *J. Geophys. Res.* **107**, A8 (2002). doi:[10.1029/2001JA900113](https://doi.org/10.1029/2001JA900113)
- Yang, L., Wu, D.J.: *Phys. Plasmas* **12**, 062903-1 (2005)